Modeling Error Evaluation of Ground Observed Vegetation Parameters

Boyi Liang [ID], Cecilia A. L. Dahlsjö [ID], Victoria Alice Maguire-Rajpaul [ID], Yadvinder Malhi [ID], and Suhong Liu [ID]

Abstract—To verify large-scale vegetation parameter measurements, the average value of sampling points from small-scale data is typically used. However, this method undermines the validity of the data due to the difference in scale or an inappropriate number of sampling points. A robust universal error assessment method for measuring ground vegetation parameters is, therefore, needed. Herein, we simulated vegetation scenarios and measurements by employing a normal distribution function and the Lindbergh–Levi theorem to deduce the characteristics of the error distribution. We found that the small- and large-scale error variations were similar among the theoretically deduced leaf area index (LAI) measurements. In addition, LAI was consistently normally distributed regardless of which a systematic error or an accidental error was applied. The difference between observed and theoretical errors was highest in the low-density scenario (7.6% at <3% interval) and was lowest in the high-density scenario (5.5% at <3% interval), while the average ratio between deviation and theoretical error of each scenario was 2.64% (low density), 2.07% (medium density), and 2.29% (high density). Furthermore, the relative difference between the theoretical and empirical errors was highest in the high-density scenario (20.0% at <1% interval) and lowest in the low-density scenario (14.9% at <1% interval), respectively. These data show the strength of a universal error assessment method, and we recommend that existing large-scale data of the study region are used to build a theoretical error distribution. Such prior work in conjunction with the models outlined in this article could reduce measurement costs and improve the efficiency of conducting ground measurements.

Index Terms—Error assessment, ground observation, leaf area index (LAI), measuring method, vegetation parameters.

I. Introduction

ESTABLISHING the connection between genotype and phenotype is currently one of the most significant chal-

B. Liang is with the College of Urban and Environmental Sciences, Peking University, Beijing 100871, China, and also with the School of Geography and the Environment, Environmental Change Institute, University of Oxford, Oxford OX1 3QY, U.K. (e-mail: liangboyi@pku.edu.cn).

C. A. L. Dahlsjö, V. A. Maguire-Rajpaul, and Y. Malhi are with the School of Geography and the Environment, Environmental Change Institute, University of Oxford, Oxford OX1 3QY, U.K. (e-mail: c.dahlsjo@gmail.com; victoria.maguirerajpaul@wolfson.ox.ac.uk; yadvinder.malhi@ouce.ox.ac.uk).

S. Liu is with the Faculty of Geography, Beijing Normal University, Beijing 100875, China (e-mail: liush@bnu.edu.cn).

lenges faced by modern plant biology [1]. Measurements of different vegetation parameters can help us understand genetic characteristics [2]. The utility and importance of terrestrial vegetation (including crops) parameters, such as leaf area index (LAI) and fractional vegetation cover (FVC), have increased in recent years [3]–[6]. There are two universally recognized methods for measuring these parameters: 1) remote sensing inversions [7]–[9] and 2) ground observations [10], [11]. Remote sensing inversion directly measures vegetation parameters at large scales (few meters to hundreds of kilometers). However, due to the technical limitations of remote sensing (relatively narrow spatial and temporal resolution, and the uncertainty of methodology), it is often necessary to cross validate these data with ground observations [12]–[14]. Meanwhile, as the extensive collection of phenotypic data remains onerous, there is often a focus on traits that are easy or inexpensive to measure, while more costly or difficult-to-score phenotypes are studied in only a few individuals [15], [16]. This approach is bound to create uncertainty when it comes to generating the true value of each vegetation parameter. In contrast to remote sensing, no universal methods for error assessments of ground observations exist. Survey costs and land accessibility limit the extent to which ground observations can be measured, so the data are normally extrapolated based on the parameters calculated for small areas [17]–[19]. For these reasons, whole regions are rarely or never measured in their entirety, which means that the sampling errors always exist.

Vegetation parameters contain two main error components [20], including a systematic error (SE) that varies between different instruments' attributes or protocols, and the accidental error made by the surveyors [21]. While probability theories, such as likelihood theory [22] and Bayes theory [23], have been used to improve existing models, the chosen error assessment must be based on appropriate specificities for each model [24]. Analytical precision can be measured by analyzing replicates or in combination with sampling precision using a balanced design of sampling and analytical duplicates. However, there are no general methods for estimating sampling bias [25]. Besides, all the previous methods for error assessment were conducted after the measurement of vegetation parameters, and we had no expectation of error distribution prior to field work [26], [27]. To address these issues, we took LAI as representative of vegetation parameters, and the aims of this study are to create an equation that can be used to estimate error distribution for ground observations and test the deduced equation on a virtual scenario using the

ground observations of LAI and compare the empirical and theoretical error distributions.

II. Deduction of Ground-Based Error Assessment

In this section, we go through the process of deduction of error distribution from normal distribution theorem and Lindeberg–Levi theorem (the latter is also known as independent distribution center limit theorem). To the best of our knowledge, this is the first time that LAI measurements have been deconstructed (true LAI, SE, and accidental error) and combined with the Lindeberg–Levi equation to achieve theoretical distribution values. Using this method, we enable error distributions to be calculated, which is important for evaluating the accuracy of vegetation parameter measurements.

The Lindeberg–Levi theorem states that when a sampling method for an independent variable (mean μ and standard deviation σ) is used, the mean tends to be normally distributed as long as the sampling size (n) is adequately large [28], [29]. This is expressed as

$$\frac{1}{n}\sum_{i=1}^{n}\xi_i \sim N\left(\mu, \frac{\sigma^2}{n}\right) \tag{1}$$

where ξ_i is each measurement, n is the number of total sampling points, and N is a normal distribution.

The LAI for each sampling point is expressed as

$$X = x + m + \varepsilon \tag{2}$$

where X is the LAI measurement for each sampling point, x is the true value of each data point (without any errors), m is the SE, and ε is the accidental error for each sampling point (irrespective of the gross error). The presence of the two errors leads to a certain degree of deviation from the value x. When ground measurements of LAI are sampled over large areas, it is likely that a variety of instruments and methods are used, which may induce SEs. We may calculate the average value of the LAI measurements with the following equation:

$$\overline{X} = \overline{x} + \frac{\sum_{i=1}^{q}m_i \times f_i}{\sum_{i=1}^{q}f_i} + \overline{\varepsilon} \tag{3}$$

where q is the different types of SEs, f_i is the number of sampling points under each SE, and m_i is the value of each SE.

According to the statistical principle of accidental error, the mean of errors would converge to zero as the sample size increases [30]. Thus, regardless of vegetation attributes, (3) may be rewritten as follows:

$$\overline{\sum_{i=1}^{q}\sum_{j=1}^{p}x_{ij}} = \overline{\sum_{i=1}^{q}\sum_{j=1}^{p}X_{ij}} - \frac{\sum_{i=1}^{q}m_i \times f_i}{\sum_{i=1}^{q}f_i} \tag{4}$$

where p is the number of sampling points for each SE. Equation (4) suggests that the difference between the true value x and the actual measured value X is equal to a weighted average of the SEs (accidental error ε is eliminated during the averaging of the values).

Based on the above-mentioned equations, we use the normal distribution theorem and Lindeberg–Levi theorem to deduce the following:

$$\frac{1}{n}\sum_{i=1}^{n}\xi_i \sim N\left(\mu - \frac{\sum_{i=1}^{q}m_i \times f_i}{\sum_{i=1}^{q}f_i}, \frac{\sigma^2}{n}\right) \tag{5}$$

where the result will follow a normal distribution based on the total sampling number (n). The mean is the true LAI minus the weighted average of the SEs, and the variation is (σ^2/n). As this deduction was based on the vegetation density and research area, the distribution and forest type will not have an impact on the results, rather it should be used as an error assessment tool. Equation (5) should be used to assess the distribution of the sampling error as well as the probability of different error intervals (deviation from true LAI) based on the variety of SEs and variation of LAI across the whole study region. If the variations of LAI at different scales are similar, we assume that the variation is the same for the whole region. In the simulated model given in the following, we test the existence of such an assumption.

III. Theoretical Validation of Error Assessment

To validate (5), we used the MATLAB software to create three scenarios with low-, medium-, and high-density vegetation levels (representing LAIs of 2.54, 5.09, and 8.09, respectively). For building a single tree, three elements, including trunk position, trunk height, and branch length, are imported. In previous studies, researchers found that the position and height of trees inhomogeneous forests tend to follow the normal and Poisson distributions, respectively [31], [32]. Based on these assumptions, we created two groups of random numbers representing tree height and tree position. Then, for each group, three numbers were randomly selected to create a low-density scenario. Meanwhile, five and eight numbers were selected in order to create a medium- and high-density scenarios, respectively. Branches (left/right) were created using (6) and (7), where the tree trunk was set perpendicular to the ground at an angle of $\alpha = \pi/2$, and the relationship between the angles of the upper branches (α_{n+1}) and the lower branches (α_n) is described as follows:

$$\alpha_{n+1}\_L = \alpha_n + pi/8$$
$$\alpha_{n+1}\_R = \alpha_n - pi/8 \tag{6}$$

where L is left and R is right. The relationship between the length of the upper branches (LOB_{n+1}) and lower branches (LOB_n) is described as follows:

$$LOB_{n+1} = 4 \times LOB_n/5. \tag{7}$$

Relevant parameters [33] were used to create three scenarios (low-, medium-, and high-density levels) using MATLAB, and each scenario includes pixels (see Fig. 1) of either vegetation or no vegetation. The true LAI for each scenario was calculated as the ratio of the number of vegetation pixels and the number of horizontal pixels in breadth.

In each scenario, the observed value of LAI was calculated by randomly selecting vertical lines, where the number of vegetation pixels that each of them contained was summed
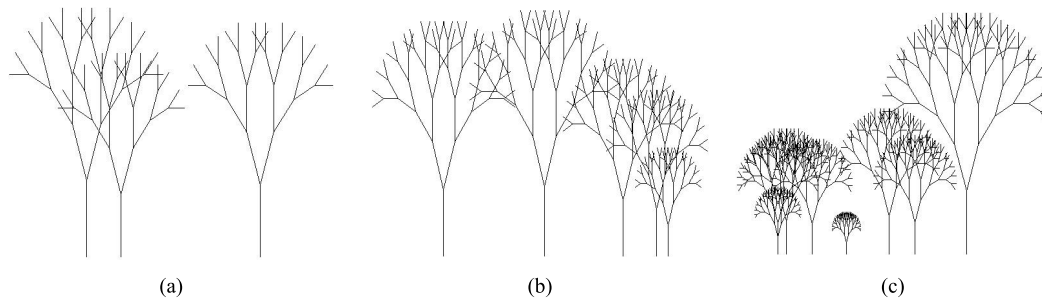
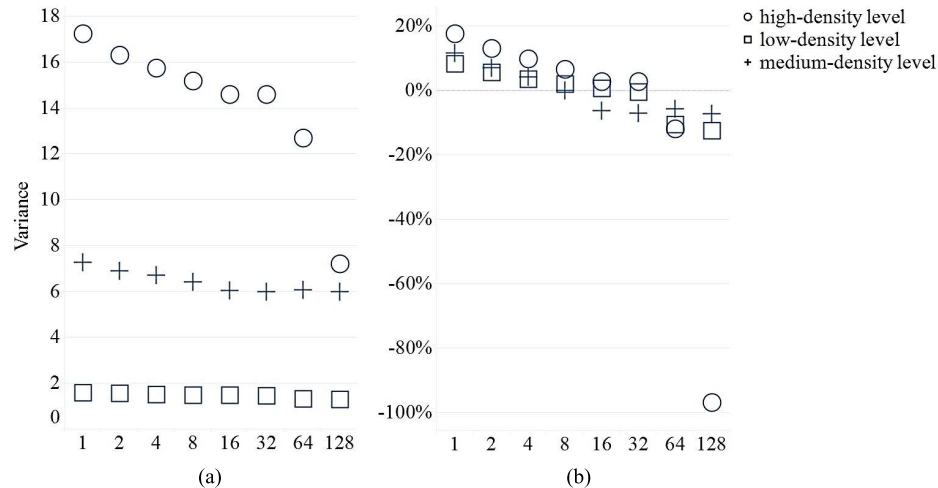Fig. 1.   Vegetation scenarios. (a) Low-density level. (b) Medium-density level. (c) High-density level.

Fig. 2.   (a) Measurement variances and (b) their anomaly with an average value at different sampling scales. There are 512 horizontal pixels in each scenario, where LAI was measured at different sampling scales (1, 2, 4, 8, 16, 32, 64, or 128 pixels, the sample scale choice was denoted as Δx).

and divided by the number of lines. Computer simulations were used to calculate the error distribution of different error intervals to verify the authenticity of the theoretical deduction.

The variation of the observed LAI was stable at certain pixel scales with the lowest variability across sampling sizes at the medium scales (see Fig. 2), suggesting that our assumption (small- and large-scale error variations are similar) was true. Based on the estimated LAI variation in the whole study region, (5) was used to calculate the error distribution of LAI measurements.

Error distribution of LAI was calculated using a sequence of the normal distribution to represent accidental error as well as five types of SE with the number of SEs ascending from 50 to 130 (see Table I). Using (5), we found that the measured average LAI was consistently normally distributed regardless of which an SE or accidental error was applied (see Fig. 3). In addition, the differences between the observed and theoretical errors were highest in the low-density scenario (7.6% difference when error interval was <3%) and lowest in the high-density scenario (5.5% difference when error interval was <3%) (see Fig. 4). The average ratio between the deviation and theoretical errors of each scenario was 2.64% (low density), 2.07% (medium density), and 2.29% (high density). The average percentage of empirical error located in one interval is, therefore, in the region of about 2% of the theoretical value.

Furthermore, the relative difference between theoretical and empirical error (when error interval was <1%) was highest in the high-density scenario (20.1% with four kinds of SE) and lowest in the low-density scenario (0.17% with one kind of SE). The average deviation from the mean between the theoretical and empirical errors in each scenario was 5.9% (low density), 4.1% (medium density), and 4.9% (high density) (see Fig. 5).

IV. DISCUSSION

In the field, different research plots often have different vegetation conditions (such as mean LAI and deviation of LAI in different subplots). However, it is hard to obtain real SE of measurements in each location. This is because SE is not only caused by different instruments but also influenced by the measuring behavior of each surveyor. For this reason, we used real data to validate error distributions that may have been created during fieldwork using different sampling sizes, excluding SE.

The data were gathered from an old secondary forest (BOB-03; 50-year postlogging, 6.69201 N, −1.307755 W) and a Savannah-forest transition plot (KOG-05, 7.30115 N, −1.164933 W) in Ghana and from an old-growth forest (NXV-02, −14.7075 S, −52.3517 W) in Brazil. LAI was measured by taking three photos (exposures −1, 0, +1) at 1-m height with a fisheye lens in each subplot (25 in each plot). The photographs were analyzed with the software Hemisfer 2.2
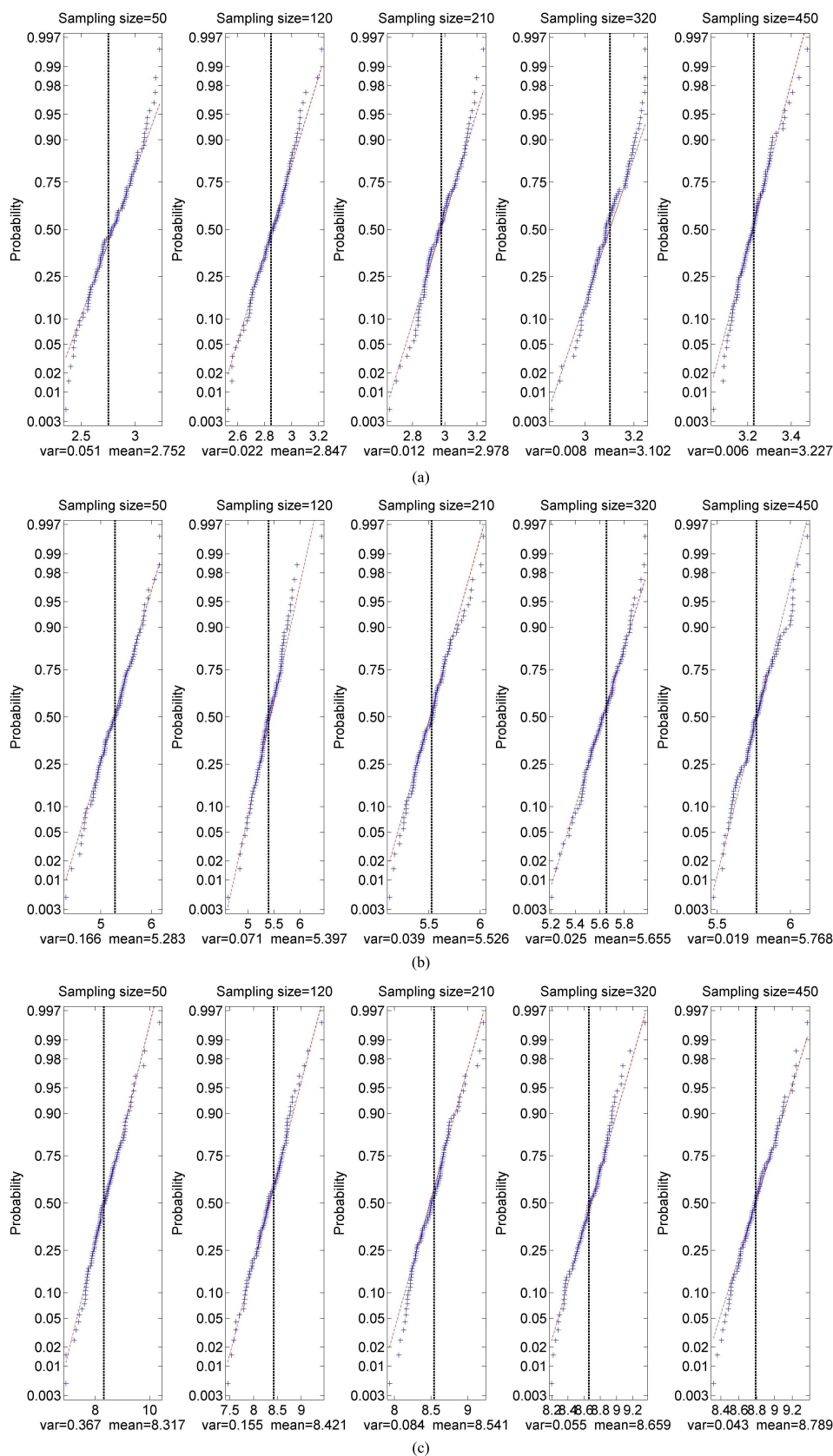
Fig. 3.   Normal distribution test of measurement results under various SEs. (a) Low-density level. (b) Medium-density level. (c) High-density level. The vertical dashed line represents the mean value of LAI, and the slanted dashed line stands for strictly normal distribution.
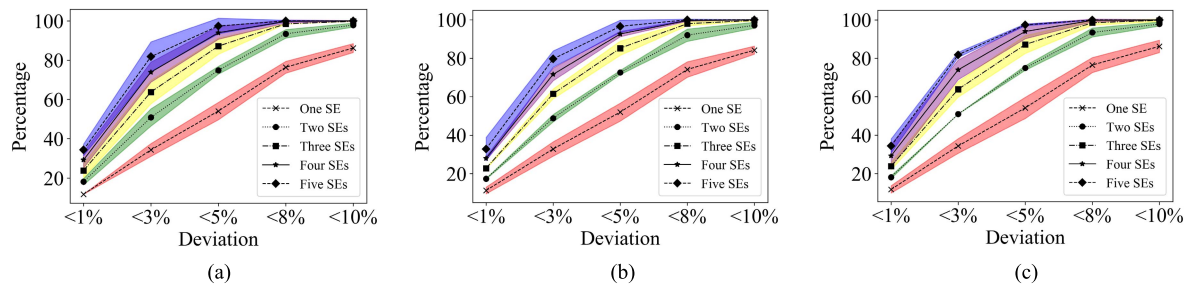
Fig. 4. Measurement error distribution. (a) Low-, (b) medium-, (c) high-density levels' SEs. Each line represents the measurement scenarios with different types of SE [j = 1, 2, 3, 4, and 5, as defined in (4)], and the abscissa stands for different ratios between deviation and theoretical LAI. For example, <1% means that the measurement result error is less than 1%. The y-axis is the percent (∗100) of sampling points in one error interval to total points. The gray area indicates the error of empirical error and the theoretical error (each dashed line). Every measurement scenario is simulated 1000 times.
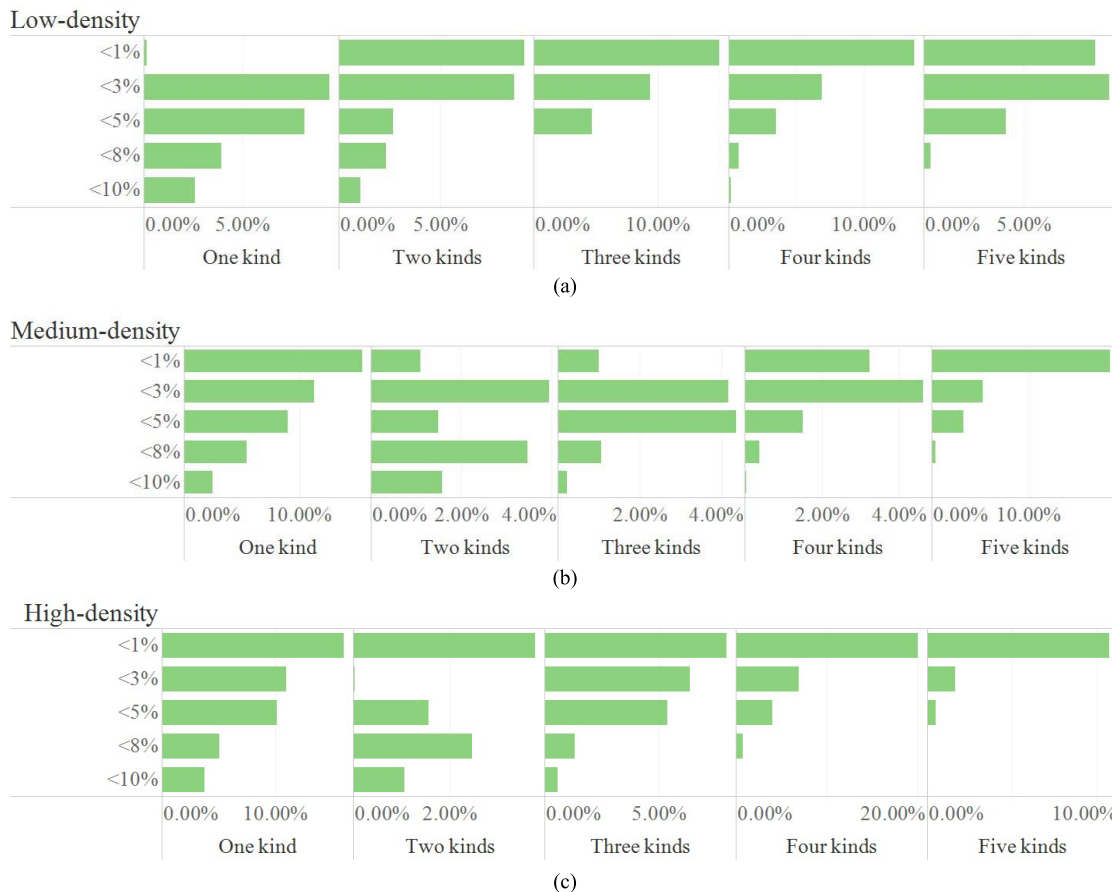

Fig. 5. Ratio between the deviation and theoretical errors at different intervals with different types of SE. (a) Low-density level. (b) Medium-density level. (c) High-density level.

(see the Supplementary Material for the details of the settings). Each plot contains 25 subplots, and the standard deviation of LAI for each plot is 0.39 (BOB-03), 0.67 (NXV-02), and 4.87 (KOG-05), respectively.

We can see in Fig. 6 that as sampling quantity increases, the results of measured LAI are closer to mean LAI (we assumed it as true value) of the plot. Meanwhile, for the plot with the highest deviation of LAI, a higher number of samples are needed in order to reduce the deviation. For example, three sampling points in BOB-03 provided a result close to mean value, while the deviation of 13 sampling points in KOG-05 was still high (about 1). The LAI in BOB-03 converged with the mean faster than in NXV-02 and KOG-05. In Fig. 6(b), the results of measurements in BOB-03 are more concentrated around the mean LAI no matter how many sampling points we used. This suggests that the sampling quantity of measurement in one research plot to reach specific error requirement should be decided by the deviation of different subplots rather than average LAI of the whole plot. This is particularly important when working with different habitat types as the forest plot in BOB-03 that has a more homogenous canopy.
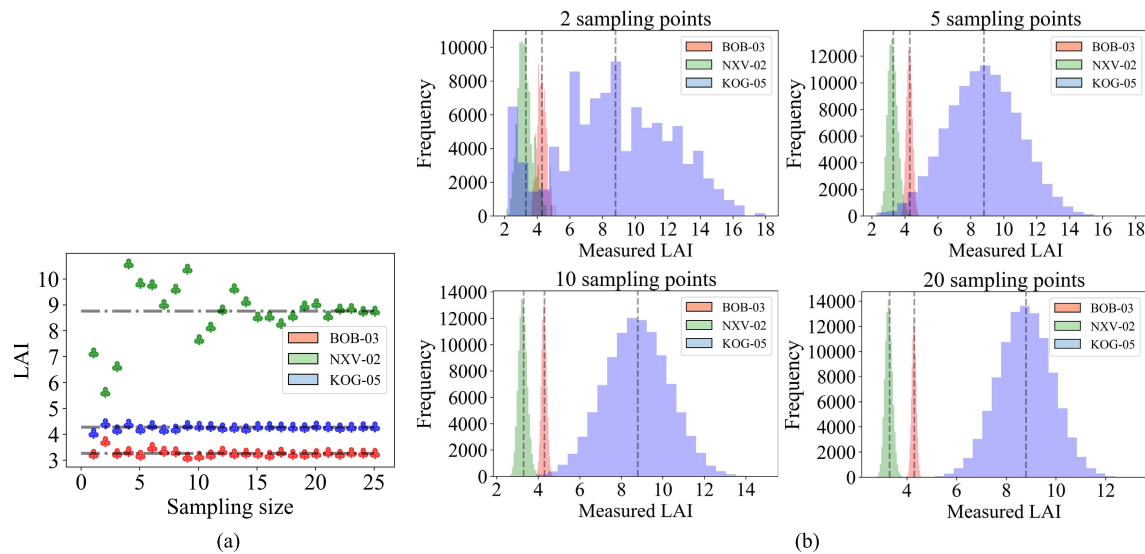
Fig. 6. Sampling result of LAI at three plots. (a) Distribution of LAI by conducting each sampling size for one time. (b) Distribution of LAI by conducting each sampling quantity 100 000 times. Gray dashed line is the average (true) LAI of subplots for each plot.

TABLE I

SE SETTING (TS: TYPES OF SE; SE: SYSTEMATIC ERROR; SN: SAMPLING SIZE). THE SYSTEM ERROR AND THE NUMBER OF SAMPLING POINTS ARE SET
ARTIFICIALLY FOR DIFFERENT TYPES OF SES. IN EACH KIND OF SE, PROGRAM ALSO SIMULATED ACCIDENTAL ERROR FOLLOWING NORMAL
DISTRIBUTION. THEORETICAL ERRORS WERE CALCULATED BY (4) AND (5)

TS	First		Second		Third		Fourth		Fifth		Theoretical error
	Se	Sn	Se	Sn	Se	Sn	Se	Sn	Se	Sn	
1	0.2	50	-	-	-	-	-	-	-	-	0.2
2	0.2	50	0.4	70	-	-	-	-	-	-	0.317
3	0.2	50	0.4	70	0.6	90	-	-	-	-	0.438
4	0.2	50	0.4	70	0.6	90	0.8	110	-	-	0.563
5	0.2	50	0.4	70	0.6	90	0.8	110	1	130	0.689

Errors occur in all geographical measurements regardless of what instruments and methods are implemented [34], [35]. In addition, both the number of sampling points and the sampling location will have an impact on the measurement output. Data collected at the small scale are often used to verify large scale data or examine the relationship between the statistical precision of sample estimates and plot size [36]–[38]. While these methods have been used as error assessments, it is now clear that measurements at different scales are likely to undermine the validity of data. For example, based on (4) and (5), when the true value of LAI in a study area is 8.09, there is a 50% chance that the deviation will be greater than 5% if the sampling size is 50. However, if the sampling size is 450, there is a high chance that the probability will be less than 5%. Therefore, better understanding and control of the error during sampling will benefit the analysis of relationships between the measured value and the true value of different vegetation parameters.

V. Conclusion

In this article, we have demonstrated the reliability and applicability of error assessment in LAI ground observations where any deviation of error distribution could be due to either the number of sampling points or the process of averaging variation across different scales. What is more, this method puts the SE and accidental error into the evaluation system, making the results more reliable.
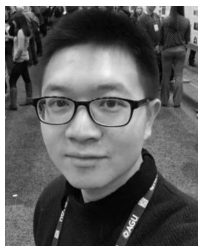
To deal with the errors that occur in the field, we should not only focus on promoting the accuracy of instruments [39], [40] and improving the authenticity of models [41], [42] but also pay attention to the distribution of errors. Overall, our error assessment method has two advantages over other models: 1) error assessment is conducted before measurement, which will give surveyors an expectation of error distribution and 2) the method has its adaptability and flexibility as theoretical error distribution for each study area is calculated by its vegetation distribution.

For future ground observed measurements, we recommend that the average variation of LAI at the large scale (e.g., using a drone or satellite imagery) is calculated or that the variation of previous vegetation parameter observations in the area is acquired. These data may thereafter be used to build a theoretical error distribution. Prior knowledge is key to produce more accurate estimates, and researchers are encouraged to have an appropriate number of sampling points to reasonably meet the error requirement. Such prior work in conjunction with the models outlined in this article could reduce the measurement costs and improve the efficiency of conducting ground measurements.

References

[1] D. Pauli *et al.*, "The quest for understanding phenotypic variation via integrated approaches in the field environment," *Plant Physiol.*, vol. 172, pp. 622–634, Sep. 2016.

[2] J. W. White *et al.*, "Field-based phenomics for plant genetics research," *Field Crops Res.*, vol. 133, pp. 101–112, Jul. 2012.

[3] A. D. Friend *et al.*, "Carbon residence time dominates uncertainty in terrestrial vegetation responses to future climate and atmospheric CO_2," *Proc. Nat. Acad. Sci. USA*, vol. 111, p. 3280, Mar. 2014.

[4] B. E. Law *et al.*, "Environmental controls over carbon dioxide and water vapor exchange of terrestrial vegetation," *Agricult. Forest Meteorol.*, vol. 113, pp. 97–120, Dec. 2002.

[5] Y. Zhang, C. Song, L. E. Band, G. Sun, and J. Li, "Reanalysis of global terrestrial vegetation trends from MODIS products: Browning or greening," *Remote Sens. Environ.*, vol. 191, pp. 145–155, Mar. 2017.

[6] J. Y. Fang, Z. D. Guo, P. Shilong, and A. P. Chen, "Terrestrial vegetation carbon sinks in China, 1981–2000," *Sci. China*, vol. 50, pp. 1341–1350, Sep. 2007.

[7] E. Grau, S. Durrieu, R. Fournier, J.-P. Gastellu-Etchegorry, and T. Yin, "Estimation of 3D vegetation density with terrestrial laser scanning data using voxels. A sensitivity analysis of influencing parameters," *Remote Sens. Environ.*, vol. 191, pp. 373–388, Mar. 2017.

[8] A. Kuusk, "Monitoring of vegetation parameters on large areas by the inversion of a canopy reflectance model," *Int. J. Remote Sens.*, vol. 19, no. 15, pp. 2893–2905, 1998.

[9] G. W. Staben, A. Lucieer, K. G. Evans, P. Scarth, and G. D. Cook, "Obtaining biophysical measurements of woody vegetation from high resolution digital aerial photography in tropical and arid environments: Northern territory, Australia," *Int. J. Appl. Earth Observ. Geoinf.*, vol. 52, pp. 204–220, Oct. 2016.

[10] J. M. Chen *et al.*, "Derivation and validation of Canada-wide coarse-resolution leaf area index maps using high-resolution satellite imagery and ground measurements," *Remote Sens. Environ.*, vol. 80, pp. 165–184, Apr. 2002.

[11] B. Liang, S. Liu, Y. Qu, and Y. Qu, "Estimating fractional vegetation cover using the hand-held laser range finder: Method and validation," *Remote Sens. Lett.*, vol. 6, no. 1, pp. 20–28, 2015.

[12] U. C. Benz, P. Hofmann, G. Willhauck, I. Lingenfelder, and M. Heynen, "Multi-resolution, object-oriented fuzzy analysis of remote sensing data for GIS-ready information," *ISPRS J. Photogramm. Remote Sens.*, vol. 58, nos. 3–4, pp. 239–258, Jan. 2004.

[13] J. E. Richey, J. M. Melack, A. K. Aufdenkampe, V. M. Ballester, and L. L. Hess, "Outgassing from Amazonian rivers and wetlands as a large tropical source of atmospheric CO_2," *Nature*, vol. 416, pp. 617–620, Apr. 2002.

[14] J. M. Chen and J. Cihlar, "Plant canopy gap-size analysis theory for improving optical measurements of leaf-area index," *Appl. Opt.*, vol. 34, no. 27, pp. 6211–6222, 1995.

[15] R. T. Furbank and M. Tester, "Phenomics-technologies to relieve the phenotyping bottleneck," *Trends Plant Sci.*, vol. 16, pp. 635–644, Dec. 2011.

[16] M. Lynch and B. Walsh, *Genetics and Analysis of Quantitative Traits*, vol. 1. Sunderland, MA, USA: Sinauer, 1998.

[17] X. Xie, W. Li, L. Lu, and M. Yang, "A new combined sampling method based on variance minimization strategy," in *Proc. Control Decis. Conf.*, 2016, pp. 1841–1844.

[18] H. Mehner, M. Cutler, D. Fairbairn, and G. Thompson, "Remote sensing of upland vegetation: The potential of high spatial resolution satellite sensors," *Global Ecology Biogeography*, vol. 13, pp. 359–369, Jun. 2010.

[19] K. L. Manies and D. J. Mladenoff, "Testing methods to produce landscape-scale presettlement vegetation maps from the U.S. Public land survey records," *Landscape Ecology*, vol. 15, pp. 741–754, Dec. 2000.

[20] M. Gottfried *et al.*, "Continent-wide response of mountain vegetation to climate change," *Nature Climate Change*, vol. 2, pp. 111–115, Jan. 2012.

[21] P. N. Morse, "A comparison of one-sided variables acceptance sampling methods when measurements are subject to error," Ph.D. dissertation, Iowa State Univ., Ames, IA, USA, 1997.

[22] F. Hartig and A. Huth, "Connecting dynamic vegetation models to data—An inverse perspective," *J. Biogeography*, vol. 39, pp. 2240–2252, Aug. 2012.

[23] H. G. Maas, A. Bienert, S. Scheller, and E. Keane, "Automatic forest inventory parameter determination from terrestrial laser scanner data," *Int. J. Remote Sens.*, vol. 29, no. 5, pp. 1579–1593, 2008.

[24] Y. Nishiyama, "Higher order asymptotic theory for semiparametric averaged derivatives," Ph.D. dissertation, London School Econ. Political Sci., London, U.K., 2001.

[25] M. H. Ramsey and A. Argyraki, "Estimation of measurement uncertainty from field sampling: Implications for the classification of contaminated land," *Sci. Total Environ.* vol. 198, no. 3, pp. 243–257, 1997.

[26] W. Bich, M. G. Cox, and P. M. Harris, "Evolution of the 'guide to the expression of uncertainty in measurement,'" *Metrologia*, vol. 43, no. 4, p. S161, 2006.

[27] M. H. Ramsey and A. A. M. Thompson, "Estimation of sampling bias between different sampling protocols on contaminated land," *Analyst*, vol. 120, no. 5, pp. 1353–1356, 1995.

[28] Q. Li and A. Ullha, "Estimating partially linear panel data models with one-way error components," *Econ. Rev.*, vol. 17, no. 2, pp. 145–166, 1998.

[29] C. Ju, T. Cai, and X. Yang, "Topography-based modeling to estimate percent vegetation cover in semi-arid Mu Us sandy land, China," *Comput. Electron. Agricult.*, vol. 64, no. 2, pp. 133–139, 2008.

[30] E. D. Ford and P. J. Newbould, "The biomass and production of ground vegetation and its relation to tree cover through a deciduous woodland cycle," *J. Ecolog.*, vol. 65, pp. 201–212, Mar. 1977.

[31] S. N. Martens, D. D. Breshears, and C. W. Meyer, "Spatial distributions of understory light along the grassland/forest continuum: Effects of cover, height, and spatial pattern of tree canopies," *Ecolog. Model.*, vol. 126, pp. 79–93, Feb. 2000.

[32] L. Breuer, K. Eckhardt, and H. G. Frede, "Plant parameter values for models in temperate climates," *Ecolog. Model.*, vol. 169, pp. 237–293, Nov. 2003.

[33] B. Liang and S. Liu, "Measurement of vegetation parameters and error analysis based on Monte Carlo method," *J. Geograph. Sci.*, vol. 28, pp. 819–832, Apr. 2018.

[34] J. R. Dymond, P. R. Stephens, P. F. Newsome, and R. H. Wilde, "Percentage vegetation cover of a degrading rangeland from SPOT," *Int. J. Remote Sens.*, vol. 13, pp. 1999–2007, Jun. 1992.

[35] S. W. Theis and A. J. Blanchard, "The effect of measurement error and confusion from vegetation on passive microwave estimates of soil moisture," *Int. J. Remote Sens.*, vol. 9, pp. 333–340, May 1988.

[36] P. Whittle, "On the variation of yield variance with plot size," *Biometrika*, vol. 43, pp. 337–343, Dec. 1956.

[37] V. K Salako, R. L. Glele Kakaï, A. E. Assogbadjo, B. Fandohan, M. Houinato, and R. Palm, "Efficiency of inventory plot patterns in quantitative analysis of vegetation: A case study of tropical woodland and dense forest in Benin," *J. South Afr. Forestry Assoc.*, vol. 75, pp. 137–143, Sep. 2013.

[38] S. Magnussen, "Effect of plot size on estimates of top height in douglasfir," *Western J. Appl. Forestry*, vol. 14, pp. 17–27, Jan. 1999.

[39] L. Brown, J. M. Chen, S. G. Leblanc, and J. Cihlar, "A shortwave infrared modification to the simple ratio for LAI retrieval in boreal forests: An image and model analysis," *Remote Sens. Environ.*, vol. 71, pp. 16–25, Jan. 2000.

[40] H. Fang, W. Li, S. Wei, and C. Jiang, "Seasonal variation of leaf area index (LAI) over paddy rice fields in NE China: Intercomparison of destructive sampling, LAI-2200, digital hemispherical photography (DHP), and AccuPAR methods," *Agricult. Forest Meteorol.*, vols. 198–199, pp. 126–141, Nov./Dec. 2014.

[41] X. Pons and L. Solé-Sugrañes, "A simple radiometric correction model to improve automatic mapping of vegetation from multispectral satellite data," *Remote Sens. Environ.*, vol. 48, no. 2, pp. 191–204, 1994.

[42] S. Sitch *et al.*, "Evaluation of ecosystem dynamics, plant geography and terrestrial carbon cycling in the LPJ dynamic global vegetation model," *Global Change Biol.*, vol. 9, no. 2, pp. 161–185, 2010.

Victoria Alice Maguire-Rajpaul's research is in human-modified tropical and savannah landscapes. Her work is focused on agriculture and on how food and forest challenges can be resiliently met with the least cost to biodiversity, ecosystem health, and tree cover. She is concerned with rural livelihoods, natural resource governance, and agricultural adaptation to climate change.

Yadvinder Malhi is currently a Professor of ecosystems science with the School of Geography and the Environment, University of Oxford, Oxford, U.K., where he is also the Program Leader of the Ecosystems Group, Environmental Change Institute, His research interests focus on understanding the functioning of ecosystems and how it is altered by processes of local and global changes. He has a particular interest in tropical forests.

Dr. Malhi is a fellow of the Royal Society and the President-Elect of the Association for Tropical Biology and Conservation.

Boyi Liang is currently a Post-Doctoral Researcher with Peking University, Beijing, China. He has worked on various programs covering modeling and forecasting of the phenological model, inversion and production of remote sensing data, and research for global vegetation growth. His research focus is on the application of remote sensing and ground observations of vegetation parameters. His main research interest is to develop mechanistic models of the relationship between phenophases and meteorological or other environmental factors using both remote sensing and field observational data in tropics.

Cecilia A. L. Dahlsjö compiles and manages Global Ecosystems Monitoring (GEM) data with a focus on the impact of the recent El Niño event. Her main interests include bottom–up approaches to ecosystem functioning and sustainable farming in the tropics. Particularly, she has been focusing on the role of decomposer organisms in both pristine and managed ecosystems around the world.

Suhong Liu is currently a Professor with Beijing Normal University, Beijing, China. Her research focus mainly includes remote sensing technology, ground observations of vegetation parameters, as well as the product of remotely sensed data (e.g., Global LAnd Surface Satellite (GLASS) leaf area index (LAI) product). Meanwhile, she has also experience in the spectral analysis of terrestrial vegetation from her previous research work.